MATERIALS SCIENCE

Liquid dispersions of zeolite monolayers with high catalytic activity prepared by soft-chemical exfoliation

Wieslaw J. Roth[1]*†, Takayoshi Sasaki[2†], Karol Wolski[1], Yeji Song[2], Dai-Ming Tang[2], Yasuo Ebina[2], Renzhi Ma[2], Justyna Grzybek[1], Katarzyna Kałahurska[1], Barbara Gil[1], Michal Mazur[3], Szczepan Zapotoczny[1], Jiri Cejka[3]

The most effective approach to practical exploitation of the layered solids that often have unique valuable properties—such as graphene, clays, and other compounds—is by dispersion into colloidal suspensions of monolayers, called liquid exfoliation. This fundamentally expected behavior can be used to deposit monolayers on supports or to reassemble into hierarchical materials to produce, by design, catalysts, nanodevices, films, drug delivery systems, and other products. Zeolites have been known as extraordinary catalysts and sorbents with three-dimensional structures but emerged as an unexpected new class of layered solids contributing previously unknown valuable features: catalytically active layers with pores inside or across. The self-evident question of layered zeolite exfoliation has remained unresolved for three decades. Here, we report the first direct exfoliation of zeolites into suspension of monolayers as proof of the concept, which enables diverse applications including membranes and hierarchical catalysts with improved access.

INTRODUCTION

Layered, two-dimensional (2D) solids consisting of weakly bonded molecularly thin nanosheets (*1*, *2*) that are exemplified by diverse valuable materials like graphite/graphene, clay minerals, metal oxides, and others with useful properties can be dispersed into suspensions of monolayers in liquids (*3*), which fulfills two functions. First, it confirms their genuinely layered nature, and second, it provides the most effective approach to practical exploitation of their useful properties to fabricate materials with particular activity and functionality (*4*). The suspended layers can be deposited on supports (*5*) or restacked into hierarchical structures alone or in combination with other compounds to produce catalysts, nanodevices, drug delivery systems, and other products with tailored properties (*6*, *7*). The significance and practical value of this process are highlighted by the recent comprehensive review (*8*), which also revealed an evident gap regarding zeolites as the newest and unexpected class of 2D solids. Zeolites are known as extremely valuable microporous 3D materials with rigid structures (*9*, *10*) but, in an unexpected twist, showed formation of layered 2D precursors (*11*–*13*) and provided unprecedented useful features: catalytically active layers with pores inside or across (*14*, *15*). Layered zeolites have not demonstrated yet the expected liquid exfoliation into monolayers (*8*, *16*). Dilute suspensions of zeolite layers covered with surfactant were obtained in low yield upon application of multistep procedures involving swelling, shearing in a melt, and purification (*5*, *15*). Both the complexity and low yield of the method thwarted broader applicability, while various alternative zeolite delamination approaches did not seem to produce any substantial verifiable exfoliation into monolayers (*17*). Here, we report facile exfoliation of the layered zeolite MCM-56 with the MWW topology, confirm unambiguously monolayer nature of the dispersions, and show the possibility for diverse practical exploitation to produce films and functional composite materials.

RESULTS AND DISCUSSION

A distinct feature of the present process is its fundamental origin involving direct soft-chemical exfoliation, in tetrabutylammonium hydroxide (TBAOH) solution, which is a standard reagent for exfoliation of various layered solids (*18*). This process is different from the alternative "liquid exfoliation" methodologies (*8*), which are often based on preswelling or mechanical cleavage. It involves massive swelling that can prop open all interlayer galleries across multilayered particles and result in total delamination/exfoliation (*19*). We prove unambiguously that MWW monolayers are the dominant component by selecting particularly revealing characterization techniques that show the following properties in sequence: expansion of the multistacked layered zeolite MCM-56 and its dispersion into monolayers [small-angle x-ray scattering (SAXS)], a layer thickness of 2.5 to 3 nm [atomic force microscopy (AFM)], preserved zeolite MWW topology and quality [in situ x-ray diffraction (XRD) and transmission electron microscopy (TEM)], flocculation, and reactions producing composite products. This combination of procedures confirms identity and high quality of the layers and can be adopted to verify and exploit exfoliation of other zeolites and 2D systems in general. We have preliminary evidence from AFM that other zeolite layers can be also dispersed by similar treatments with TBAOH, which indicates that this method is general, as expected from the fundamental principles and definition of 2D materials.

Zeolite MCM-56 (*20*–*22*), which produced the reported monolayer dispersion directly by treatment with TBAOH solutions, is one of the seven distinct forms, mostly layered, of the framework MWW obtained by direct synthesis (*23*). It is a unique delaminated zeolite synthesized directly that can be identified by powder XRD in the range 5° to 10° 2θ (Cu Kα radiation, used throughout; λ = 0.15405 nm) showing a relatively sharp 100 peak at 7.1° 2θ and a broad band between 8° and 10° 2θ indicating disordered layer packing (*24*). It matches simulated XRD patterns for single MWW layers (*15*, *21*),

[1]Faculty of Chemistry, Jagiellonian University, Gronostajowa 2, 30-387 Kraków, Poland. [2]International Centre for Materials Nanoarchitectonics (WPI-MANA), National Institute for Materials Science (NIMS), 1-1 Namiki, Tsukuba, Ibaraki 305-0044, Japan. [3]Department of Physical and Macromolecular Chemistry, Faculty of Sciences, Charles University, Hlavova 8, 128 43 Prague 2, Czech Republic.
*Corresponding author. Email: wieslaw.roth@uj.edu.pl
†These authors contributed equally to this work.

which are 2.5 nm thick and contain <0.3-nm-wide perpendicular channels (6-member Si-O rings), internal pores with a diameter of ca. 0.55 nm, and surface cavities of ca. 0.7 nm wide and deep. MCM-56 is intrinsically very acidic due to high Al concentration (Si/Al~10), and the as-synthesized form contains 15% of hexamethyleneimine (HMI) (*20*).

The discovered exfoliation that we report here was effective with a particular MCM-56 formulation (and possibly some others too), affording yields up to 40% (0.2 g from a typical preparation starting from 0.5 g of MCM-56). The dispersion into independent 2.5-nm-thick monolayers was first confirmed by AFM, as we show below, but we will present the evidence sequentially starting from bulk measurements. SAXS examination confirmed expansion of MCM-56 in 6 to 10% TBAOH solutions (fig. S1), indicated by distinct peaks due to regular stacking of layered structures, with gradually increasing basal spacing from 5.3 to 6.2 nm as the TBAOH concentration decreased. These spacings correspond to 2.8- to 3.7-nm interlayer space enlargement, which is much larger than 1.1 nm diameter of TBA^+ cations. This is consistent with the behavior of metal oxides including titanates and is defined as osmotic swelling (*25*). No interlayer peaks were detected in 4% TBAOH, suggesting disintegration of the layered structure, i.e., exfoliation.

Colloidal suspensions of MWW monolayers could be produced directly by stirring MCM-56 with 3 to 5% TBAOH solutions, in accordance with the SAXS experiments, but it was more convenient to study suspensions prepared by a two-step process with much lower final TBAOH concentration of ca. 0.01 M. In the first step, we contacted MCM-56 with 10 to 11% TBAOH, 1:50 (w/w) ratio, for approximately 2 hours, centrifuged at 10,000 rpm, and obtained a solid and clear supernatant, which we decanted. We stirred the wet solid with pure water and obtained translucent colloid of MWW monolayers, which we characterized by physical methods and isolated as composites with useful potential as described below (*17*, *26*, *27*).

We confirmed the overwhelmingly monolayer nature of the colloids by in situ XRD of the gel-like solid containing concentrated layers (see Materials and Methods; figs. S2 and S3). We obtained this solid by centrifugation at 15,000 rpm for 30 min. The XRD pattern showed wavy and broad profile, which matched well with the square of the calculated layer structure factor (Fig. 1) (*18*, *25*), proving essentially total exfoliation.

If the sample contained unexfoliated stacks of zeolite layers, then the pattern would show basal diffraction series. The broad and continuous profile, which matched with the square of the layer structure factor, indicates that the MWW layers scatter x-rays individually and that no interference occurs. The profile in Fig. 1 is different from the previously reported data for MWW monolayers, showing in-plane peaks and broad features from out-of-plane scattering (*15*, *21*). This difference is caused by the fact that we collected our XRD data from concentrated layers oriented parallel to the XRD holder (fig. S2). In other words, the scattering vector of the measurement was parallel to the layer normal or *c* axis of the zeolite layer. In this case, only the atomic positions, z_j, along the layer normal involve the x-ray scattering. In contrast, the previously reported data were recorded from samples in which the layers were oriented randomly.

As mentioned above, the monolayer nature was evident in the AFM height profiles, shown in Fig. 2, of diluted, spin-coated colloid samples. The images and histograms showed layers predominantly 2.5 nm in height, consistent with the crystallographic c-unit cell of the MWW zeolite. The average content of monolayers calculated from eight AFM height images (10 μm square each) was 83 ± 5%, but it might be higher in the suspension or can possibly be increased. The rest were double layers. We obtained similar results with undiluted suspensions.

We evaluated the exact structure and quality of the dispersed monolayers by in-plane XRD and TEM (Fig. 3), which showed highly ordered and crystalline materials with MWW topology. In-plane scattering (fig. S4) showed sharp peaks that could all be indexed on the 2D hexagonal cell with refined $a = 1.482(1)$ nm, which is similar to the typical lattice constant for the MWW materials MCM-22 and MCM-49 equal to 1.43 nm (*28*). The observed nominal difference may be due to high content of Al, which is known to expand zeolite lattices. This proved that the MWW structure and 2D atomic architecture remained unchanged.

The TEM image of an exfoliated nanosheet (Fig. 3A) revealed regular hexagonal patterns of cavities, extended to the whole nanosheet. The corresponding selected area electron diffraction (SAED) pattern (Fig. 3B) could be indexed as a single crystalline MWW structure

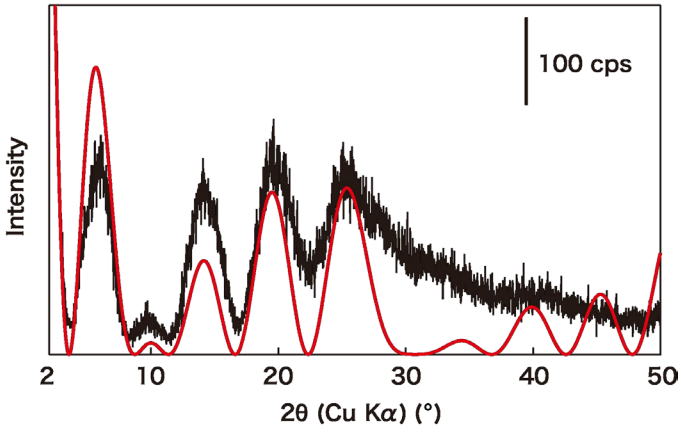

Fig. 1. In situ XRD of concentrated layers in water (black line) and the square of structure factor F (red line) calculated based on the MWW structure. The observed deviation between the calculated and experimental intensities at higher 2θ angles is due to amorphous halo from water because the glue-like sample recovered via centrifugation contains large amount of the solvent. Damping the wavy profile at a higher angular range may be involved by some structural disorder.

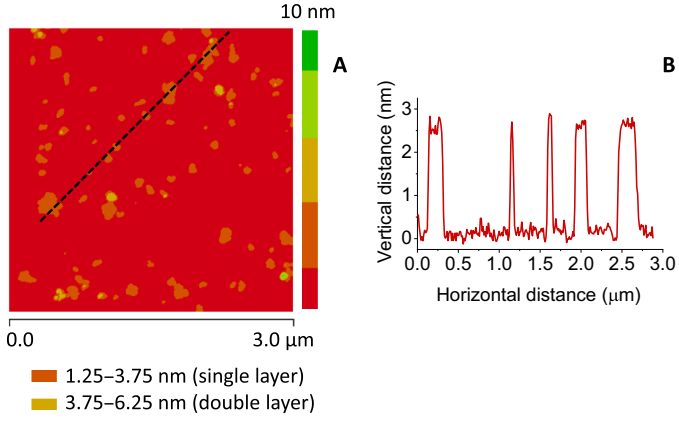

Fig. 2. AFM topography image of diluted colloidal MCM-56. Zeolite suspension deposited on a silicon support modified with polyethylenimine (PEI) solution (**A**) and height profile along the marked line (**B**).

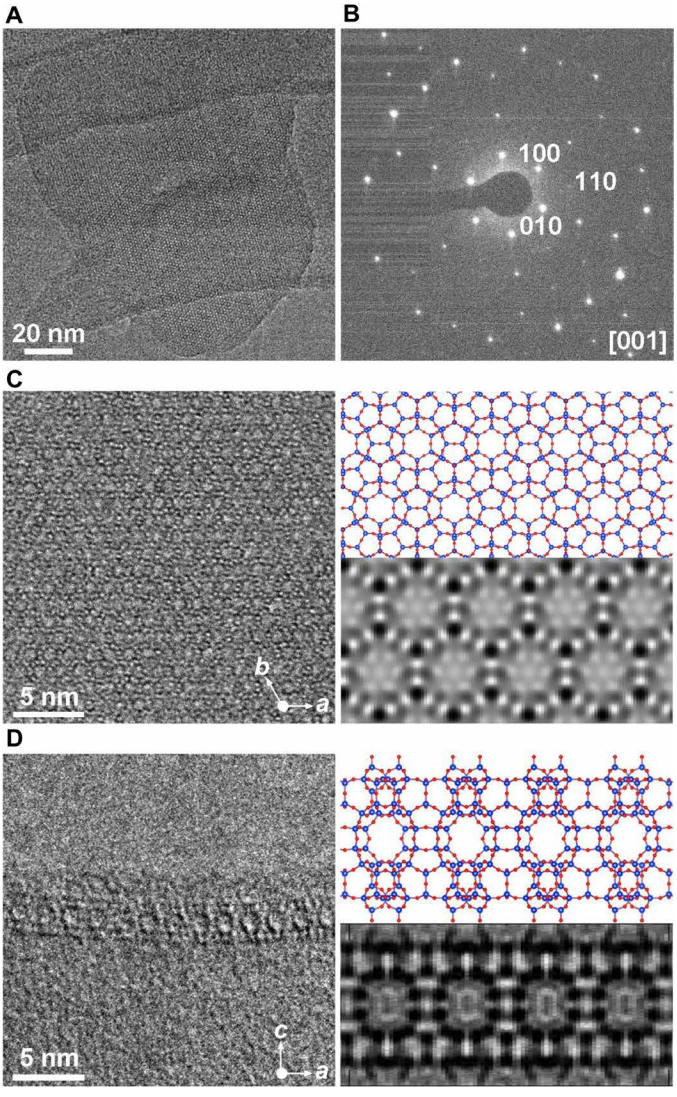

Fig. 3. Crystalline structure of MCM-56 monolayers separated from the colloidal suspensions. (**A** and **B**) TEM image and SAED pattern along the c-axis, showing the whole nanosheet to be a single crystal. (**C** and **D**) HRTEM images, atomic models, and simulated TEM images of in-plane (C) and edge-view (D) structures.

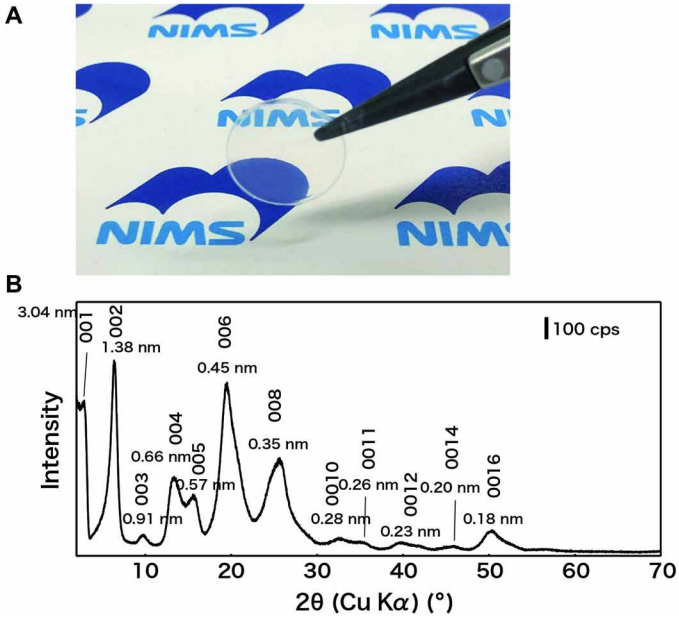

Fig. 4. Zeolite film with a diameter of 18 mm obtained from the colloidal dispersion. (**A**) photograph and (**B**) XRD data, which show only the basal reflections and no peaks associated with the in-plane periodicity, confirming that zeolite nanosheets are stacked with their faces parallel to the film surface. Photo credit: Yeji Song, NIMS.

along the [001] zone axis. High-resolution TEM (HRTEM) images further demonstrate fine structures for both in-plane (Fig. 3C) and edge-on (Fig. 3D) orientations that are consistent with the simulated TEM image from the atomic model. The side-view TEM image clearly shows that the nanosheet has a thickness of one unit cell with evident ellipsoidal pores. These results prove that the regular porous and crystalline structure of the exfoliated monolayers were well preserved, as was also observed in precipitated MWW layer surfactant composites discussed below (fig. S6).

The obtained colloids have inherent practical value, due to zeolitic nature, which can be exploited in many ways. We illustrate their potential here by showing the formation of self-standing films and intimate composite materials with separated layers that can include additional active components. We fabricated a self-standing and transparent film of the zeolite nanosheets simply by filtering the dispersion through a millipore filter (Fig. 4 and fig. S5). In the film, the nanosheets are oriented parallel to the film surface, which we confirm by XRD data showing a series of basal peaks corresponding to d = 2.7 to 2.8 nm (the peaks are not perfectly rational because of a limited number of the stacked sheets) (*29*, *30*). This may be the first demonstration of oriented zeolite films, which can only be produced from a dispersion of delaminated nanosheets. We expect various possible applications for these films, e.g., as filtering or desalination membranes and catalysts. These dispersions can be also used for deposition of monolayers to produce zeolite membranes, but it is difficult to imagine that continuous films, which are highly desirable, can be obtained this way directly. As a possible solution, Tsapatsis *et al.* (*15*) demonstrated secondary growth of additional zeolite framework to "fill the gaps." The present nanosheets have the advantage by appearing to be "bare" except for TBA^+ cations, which should be easy to displace. Previously, only functionalized zeolite monolayers with attached surfactant were available (*5*, *17*), which added another level of complexity through the need to remove strongly adhering hydrophobic organics (surfactant).

We illustrate the preparation of composite products in bulk, which can be used to introduce additional active components and/or to design structures, by flocculation reactions that occur upon mixing the colloids with suitable reactants. The examples we present here (fig. S6) include flocculation with cationic surfactant, hexadecyltrimethylammonium chloride (HDTMA-Cl), producing equivalent of the surfactant-swollen MWW zeolite, and with the Al-oxo cluster, $(Al_{13}O_4(OH)_{24}(H_2O)_{12})^{7+}$, (Al-oxo-13), which initiated the practice of pillaring layered solids as molecular sieves with increased pore sizes (*31*). The reaction with surfactant, HDTMA-Cl, represents chemical evidence that MWW monolayers are the predominant component in the colloids. The product was similar, according to XRD (fig. S6), to a swollen multilayered MWW with d-spacing around 5 nm (*32*). It could form only from monolayers because multilayered MWW particles, if present, would not be swollen by the surfactant under these conditions, as it requires high pH of >0.3 M hydroxide (*24*, *33*). The surfactant-MWW

composite that we obtained by the colloid route is notable for its particularly intense diagnostic 003 XRD reflection, at approximately 5° 2θ, suggesting high extent of swelling and quality (*24*, *33*), which can be useful for additional transformation, e.g., into pillared products.

The reaction between MWW colloids and the Al-oxo-13 cluster produced materials, which could not be obtained otherwise, e.g., by ion exchange or pillaring of swollen derivatives (*27*). The obtained products contained, as expected (*27*), both micro- and mesopores. They showed an unusual hysteresis-related feature in the nitrogen sorption isotherm, namely, a double-step desorption at $p/p_0 > 0.5$, observed previously in plugged SBA-15 mesoporous materials with both open and blocked cylindrical mesopores (*34*). The behavior of these systems during preparation and ensuing properties are more complex than in a simple pillaring. It needs more detailed studies and is probably complicated by the pH-dependent reactivity of the Al-oxo-13 species in solution.

Zeolitic layers are very attractive candidates for preparation of more open, improved catalysts with increased access to active sites. MWW zeolites are high activity catalysts used in industrial aromatic alkylation (*35*). The product we isolated after the exfoliation procedure showed slightly increased porosity (fig. S6 and table S1), lower Brønsted acid site concentration, and higher Lewis acid site content in comparison to the parent MCM-56 (table S1). Despite this adverse impact on acid properties, the performance of this catalyst was comparable to the original zeolite in a model mesitylene benzylation reactions tailored for testing surface activity (fig. S7). This is already a notable positive outcome in view of the concerns that individual zeolite layers may be susceptible to coiling or other forms of degradation or deactivation (*15*). Improvements can now be pursued by stabilization of acid sites, functionalization of the layers, and design of structures with larger interlayer spaces.

In summary, the evidence of essentially total exfoliation that we report here removes the formal difference between 2D zeolites and the other layered materials. It presents unique opportunities for preparation of functional materials, e.g., with mixed layers, and provides enticement for exfoliation of other zeolite structures, as they can provide different kinds of activity. As we mentioned above, positive results have been already obtained with other zeolites to confirm the general nature of the reported phenomena and processes with applicability to all truly layered zeolite materials.

MATERIALS AND METHODS

Synthesis methods

Synthesis of MCM-56

The preparation was based on the published procedure (*20*) using the following reagents (from Sigma-Aldrich, except for sodium aluminate): 50% NaOH, sodium aluminate (40 to 45% Na_2O and 50 to 56% Al_2O_3; Riedel-de-Haen), sources of silica (nanopowder with a particle size of 10 to 20 nm or fumed silica; Aerosil), HMI (98%), and deionized water with the molar ratios (1 SiO_2:0.04 Al_2O_3:0.093 Na_2O:0.3 HMI:16 H_2O). The mixture was rotated in a Teflon-lined autoclave overnight at room temperature and then heated at 145°C with rotation for 38 hours. The solid was isolated by filtration, washed with deionized water, and dried at room temperature.

Preparation of colloidal suspensions

Typically, the exfoliation was carried out with 0.5 g of MCM-56 stirred for 2 hours or longer with 27 g of 11% TBAOH. The rate of stirring was of the order of several hundred revolutions per minute (rpm) and varied depending on the type of magnetic stirrer used. Following centrifugation at 10,000 rpm for 20 to 30 min, the clear supernatant was decanted as much as possible, and 14 ml of water was added. Stirring of the mixture for 1 to 2 hours produced translucent liquid. Residual solid was removed by centrifugation at 10,000 rpm for 20 min or more, and the colloid was separated by decantation. Additional but less concentrated colloidal suspension could be obtained by adding water to the solid residue, stirring, and centrifugation.

Reaction with surfactant

The colloid was mixed with 3 to 4 volumes of 25% HDTMA-Cl solution (Sigma-Aldrich), which produced immediate white precipitate. It was isolated by centrifugation at 10,000 rpm for 10 to 20 min, slurried with 5 to 10 ml of water after decantation, and centrifuged again. The solid was dried at 60°C overnight.

Reaction of the colloid with Al-oxo-13 cluster ion solution

A monolayer suspension obtained according to the procedure above was added dropwise with stirring into 3 g of commercial sample of aluminum chlorhydrol in 100 ml of water. Fine precipitate formed immediately. The slurry was stirred overnight, and the solid was isolated by centrifugation at 10,000 rpm for 10 min. The obtained product was washed with 10 ml of water, dried at room temperature for several days, and calcined at 540°C for 6 hours.

Characterization

X-ray powder diffraction

The patterns were collected with a step of 0.02° using a Bruker D2 Phaser diffractometer with settings 10 mA and 10 kV and a Rigaku MiniFlex diffractometer in reflection mode; the radiation was Cu Kα (λ = 0.15405 nm).

Low-temperature nitrogen adsorption, in situ Fourier transform infrared spectroscopy, x-ray fluorescence, and catalytic testing

Low-temperature nitrogen adsorption, in situ Fourier transform infrared spectroscopy, x-ray fluorescence, and catalytic testing were performed by standard procedures as previously described in detail (*23*).

Small-angle x-ray scattering

A sample of the original MCM-56 (0.1 g) was reacted with TBAOH solutions (6 ml) at varied concentrations for 2 days. Then, the swollen sample in the solution (50 to 100 μl) was gently pipetted out, transferred to a hollow slit with a depth of 2 mm in the sample holder, and thoroughly sealed with Scotch tape. A Rigaku NANO-Viewer with Cu Kα radiation was used to record the SAXS signal with a total measuring time of 2 hours. The alignment of SAXS axes is calibrated periodically, every other month, to avoid the zero shift.

Atomic force microscopy

The reagents used for sample preparation were obtained from the following sources: branched polyethylenimine (PEI; molecular weight, ~600 g/mol) was purchased from Sigma-Aldrich, and toluene (pure for analysis, p.a.), tetrahydrofuran (THF) (p.a.), ethanol (p.a.), NaCl (p.a.), H_2SO_4 (96%), and H_2O_2 (30%) were purchased from Chempur. All reagents were used as received.

Silicon wafers were sonicated in ethanol for 10 min, dried, and placed in piranha solution (H_2SO_4:H_2O_2, 3:1) for 15 min at room temperature. Afterward, the plates were rinsed with copious amounts of deionized water, THF, and toluene and dried in the stream of argon. These prepared substrates were then treated with hand-held atmospheric plasma cleaner (Plasma Wand, Plasma Etch, Carson City, Nevada, USA) for 60 s and subsequently placed in the glass vials with PEI solution (1 g/liter) in 0.01 M NaCl. PEI deposition was supported by pulse sonication (15 min). After completion, the samples

were rinsed with copious amount of deionized water and dried in the stream of argon. Last, the diluted colloid solution (150-fold) was spin-casted (2000 rpm, 120 s) on the PEI-modified support.

AFM images were obtained with a Dimension Icon AFM (Bruker, Santa Barbara, CA) working in the PeakForce Tapping and QNM (Quantitative Nanomechanical Mapping) modes. AFM probes (TESPA, Bruker) probes with a nominal spring constant of 42 N/m were used for all measurements. The total surface coverage and the percentage of single layer structure (image area occupied by single layer structure/total surface area covered with sample) were calculated using bearing analysis. The images were captured in eight different places on the sample (resolution, 384 × 384; size, 10 μm by 10 μm for bearing analysis and 3 μm by 3 μm for analysis of topography).

In situ XRD

The in situ XRD data were collected after the colloidal suspension was subjected to high-speed centrifugation at 15,000 rpm for 30 min to recover a glue-like sediment of concentrated layers. This wet sample was loaded onto the XRD sample holder, and its diffraction pattern was recorded. The measurements were carried out at 30°C and high relative humidity (RH) of 95% using a specially designed diffractometer (RINT-Ultima) to avoid sample drying (fig. S2). The RH in the sample chamber of the diffractometer was regulated by circulating dry and moisture-saturated N_2 gas at a specified ratio. XRD measurement was conducted using graphite-monochromatized Cu Kα radiation (λ = 0.15405 nm) with a step of 0.02° and a scan speed of 1°/min.

The XRD profile was simulated assuming that the nanosheets lie parallel to the sample holder (fig. S2). This is the most likely orientation, considering the highly 2D anisotropic morphology of the layers and the pressing action to obtain the flat surface of the glue-like sample. In this alignment, the pattern is expected to correspond to the square of layer structure factor *F*, which can be calculated according to the following Eq. 1 (*36*)

$$F = \sum_j n_j f_j \exp\left(2\pi i\left(2 z_j \frac{\sin\theta}{\lambda}\right)\right) = 2\sum_j n_j f_j \cos\left(2\pi\left(2 z_j \frac{\sin\theta}{\lambda}\right)\right) \quad (1)$$

where n_j, f_j, θ, and λ are the number of atoms, atomic scattering factors, diffraction angles, and x-ray wavelength, respectively. The atomic positions, z_j, along the layer normal were derived from the MWW structure with 72 T sites with averaged *f* (0.9Si + 0.1 Al) and 144 oxygen atoms (fig. S3) (*10*). We exclude Na ions and organic moieties considering their substantially negligible scattering. Because the MWW layer is centrosymmetric, the atoms located at 0 to 0.5 are taken into account.

TEM imaging of MWW layers

MCM-56 colloid suspension was drop-casted onto a Cu TEM grid covered with a lacey carbon film. TEM observations and SAED patterns were performed using a JEOL 3100FEF (accelerating voltage, 300 kV), with a Gatan UltraScan 1000 charge-coupled device camera (2048 pixels × 2048 pixels). The camera length for SAED was 60 cm. To reduce the electron beam irradiation damage because of beam sensitivity of 2D zeolites, a low-dose condition was adopted by using a small spot size (no. 5) and a small condenser lens aperture (CLA-3) so that the dose was limited to ~200 electrons/$Å^2$ for capturing one image. In addition, the atomic structure was characterized by using a JEM-ARM200F (accelerating voltage, 80 kV) equipped with a Cs corrector (CEOS). HRTEM image simulations were conducted by using quantitative TEM/STEM (QSTEM) software developed by Koch (*37*). For comparison of the experimental and simulated TEM images, the focus was set to the Scherzer defocus condition.

In-plane XRD

A silicon wafer (1 cm by 4 cm) was cleaned by immersing in methanol/HCl mixture (1:1 in volume) and subsequently in concentrated H_2SO_4 for 30 min. After rinsing thoroughly with deionized (Milli-Q) water, the wafer was immersed in an aqueous solution of PEI [0.025 g/liter (pH = 9)] for 15 min to introduce positive charge onto the surface. After washing with copious amounts of water, the PEI-primed Si substrate was vertically dipped into MCM-56 colloidal suspension for 10 min. The wafer was dried by blowing with N_2 gas. AFM analysis revealed that the nanosheets lie on the substrate as a monolayer film. In-plane XRD data were collected using synchrotron radiation x-rays (λ = 0.11971 nm) at the Photon Factory, BL-3A, KEK.

Fabrication of zeolite films

A self-standing film was fabricated on the membrane filter (MF-Millipore, mixed cellulose esters, with a pore size of 0.025 mm) by filtration. The colloidal suspension was centrifuged (20,000 rpm, 30 min) to produce a top solution and a sediment. After discarding the solution, the solid was redispersed. This procedure was repeated twice to reduce the TBAOH concentration. A 3-ml aliquot of the obtained colloid was filtered by dry pump for 5 hours to dry both the zeolite film and membrane filter. The cross-sectional image was observed with field-emission SEM (Hitachi, S-4800), and XRD data were collected using Rigaku UltimaIV with graphite-monochromatized Cu Kα radiation (λ = 0.15405 nm) with a step of 0.02° and a scan speed of 0.1°/min.

TEM of the surfactant-MWW composite

TEM imaging was performed using JEOL NEOARM 200 F with a Schottky-type field emission gun at an accelerating voltage of 200 kV. The microscope was equipped with TVIPS XF416 CMOS camera. The alignment was performed using standard gold nanoparticles film method. Because of the low beam stability of the sample, the dose of electrons was kept below a current density of 2 pA/cm^2.

SUPPLEMENTARY MATERIALS

Supplementary material for this article is available at http://advances.sciencemag.org/cgi/content/full/6/12/eaay8163/DC1

Fig. S1. SAXS profiles for MCM-56 samples in TBAOH solutions at different concentrations (10, 8, 6, and 4 weight %).

Fig. S2. Graphical illustration of the in situ XRD setup and measurement.

Fig. S3. The atomic positions used in structure factor calculation for the MWW layer.

Fig. S4. In-plane XRD data for monolayers from the MCM-56 colloid deposited onto a Si substrate.

Fig. S5. Photographs and cross-sectional SEM images of the MWW zeolite film produced from the colloidal suspension of MCM-56 layers.

Fig. S6. Selected powder XRD, TEM, and nitrogen adsorption/desorption characteristics of the materials obtained from the MCM-56 colloid suspensions.

Fig. S7. Catalytic activity of the original MCM-56 and the zeolite recovered from colloid by flocculation with 1 M ammonium nitrate: Conversion of benzyl alcohol in alkylation of mesitylene.

Table S1. Representative acidic and textural properties of the starting MCM-56 zeolites and the products obtained from the colloidal dispersions by flocculation with 1 M ammonium nitrate solution and the Al-oxo-13 cluster ions.

REFERENCES AND NOTES

1. G. Alberti, U. Constantino, Layered solids and their intercalation chemistry, in *Comprehensive Supramolecular Chemistry*, J. L. Atwood, J. E. D. Davies, D. D. MacNichol, F. Vogtle, Eds. (Pergamon, 1996), vol. 7, pp. 1–23.
2. D. O'Hare, Inorganic Intercalation Compounds, in *Inorganic Materials*, D. W. Bruce, D. O'Hare, Eds. (Wiley, 1997), pp. 172–254.
3. A. J. Jacobson, Colloidal dispersions of compounds with layer and chain structures. *Mater. Sci. Forum* **152-153**, 1–12 (1994).

4. K. S. Novoselov, D. Jiang, F. Schedin, T. J. Booth, V. V. Khotkevich, S. V. Morozov, A. K. Geim, Two-dimensional atomic crystals. *Proc. Natl. Acad. Sci. U.S.A.* **102**, 10451–10453 (2005).
5. K. V. Agrawal, Towards the ultimate membranes: Two-dimensional nanoporous materials and films. *Chimia* **72**, 313–321 (2018).
6. R. Ma, T. Sasaki, Two-dimensional oxide and hydroxide nanosheets: Controllable high-quality exfoliation, molecular assembly, and exploration of functionality. *Acc. Chem. Res.* **48**, 136–143 (2014).
7. M. Osada, T. Sasaki, Nanosheet architectonics: A hierarchically structured assembly for tailored fusion materials. *Polym. J.* **47**, 89–98 (2015).
8. V. Nicolosi, M. Chhowalla, M. G. Kanatzidis, M. S. Strano, J. N. Coleman, Liquid exfoliation of layered materials. *Science* **340**, 1226419 (2013).
9. A. F. Masters, T. Maschmeyer, Zeolites - From curiosity to cornerstone. *Micropor. Mesopor. Mat.* **142**, 423–438 (2011).
10. International Zeolite Association, Database of Zeolite Structures (2017); www.iza-structure.org/databases/.
11. M. E. Leonowicz, J. A. Lawton, S. L. Lawton, M. K. Rubin, MCM-22: A molecular sieve with two independent multidimensional channel systems. *Science* **264**, 1910–1913 (1994).
12. L. Schreyeck, P. Caullet, J. C. Mougenel, J. L. Guth, B. Marler, PREFER: A new layered (alumino) silicate precursor of FER-type zeolite. *Micropor. Mat.* **6**, 259–271 (1996).
13. W. J. Roth, P. Nachtigall, R. E. Morris, J. Čejka, Two-dimensional zeolites: current status and perspectives. *Chem. Rev.* **114**, 4807–4837 (2014).
14. M. Choi, K. Na, J. Kim, Y. Sakamoto, O. Terasaki, R. Ryoo, Stable single-unit-cell nanosheets of zeolite MFI as active and long-lived catalysts. *Nature* **461**, 246–249 (2009).
15. K. Varoon, X. Y. Zhang, B. Elyassi, D. D. Brewer, M. Gettel, S. Kumar, J. A. Lee, S. Maheshwari, A. Mittal, C.-Y. Sung, M. Cococcioni, L. F. Francis, A. V. McCormick, K. A. Mkhoyan, M. Tsapatsis, Dispersible exfoliated zeolite nanosheets and their application as a selective membrane. *Science* **334**, 72–75 (2011).
16. W. J. Roth, B. Gil, W. Makowski, B. Marszalek, P. Eliášová, Layer like porous materials with hierarchical structure. *Chem. Soc. Rev.* **45**, 3400–3438 (2016).
17. A. Corma, V. Fornes, S. B. Pergher, T. L. M. Maesen, J. G. Buglass, Delaminated zeolite precursors as selective acidic catalysts. *Nature* **396**, 353–356 (1998).
18. R. Ma, T. Sasaki, Nanosheets of oxides and hydroxides: Ultimate 2D charge-bearing functional crystallites. *Adv. Mater.* **22**, 5082–5104 (2010).
19. L. Wang, T. Sasaki, Titanium oxide nanosheets: Graphene analogues with versatile functionalities. *Chem. Rev.* **114**, 9455–9486 (2014).
20. W. J. Roth, P. Chlubná, M. Kubů, D. Vitvarová, Swelling of MCM-56 and MCM-22P with a new medium - surfactant-tetramethylammonium hydroxide mixtures. *Catal. Today* **204**, 8–14 (2013).
21. G. G. Juttu, R. F. Lobo, Characterization and catalytic properties of MCM-56 and MCM-22 zeolites. *Micropor. Mesopor. Mat.* **40**, 9–23 (2000).
22. W. J. Roth, MCM-22 zeolite family and the delaminated zeolite MCM-56 obtained in one-step synthesis, in *Molecular Sieves: From Basic Research to Industrial Applications*, J. Čejka, N. Žilková, P. Nachtigall, Eds. (Elsevier, 2005), vol. 158A and B, pp. 19–26.
23. J. Grzybek, W. J. Roth, B. Gil, A. Korzeniowska, M. Mazur, J. Čejka, R. E. Morris, A new layered MWW zeolite synthesized with the bifunctional surfactant template and the updated classification of layered zeolite forms obtained by direct synthesis. *J. Mater. Chem. A* **7**, 7701–7709 (2019).
24. W. J. Roth, J. Čejka, R. Millini, E. Montanari, B. Gil, M. Kubu, Swelling and interlayer chemistry of layered MWW zeolites MCM-22 and MCM-56 with high Al content. *Chem. Mater.* **27**, 4620–4629 (2015).
25. T. Sasaki, M. Watanabe, Osmotic swelling to exfoliation. Exceptionally high degrees of hydration of a layered titanate. *J. Am. Chem. Soc.* **120**, 4682–4689 (1998).
26. M. Y. Jeon, D. Kim, P. Kumar, P. S. Lee, N. Rangnekar, P. Bai, M. Shete, B. Elyassi, H. S. Lee, K. Narasimharao, S. N. Basahel, S. Al-Thabaiti, W. Xu, H. J. Cho, E. O. Fetisov, R. Thyagarajan, R. F. DeJaco, W. Fan, K. A. Mkhoyan, J. I. Siepmann, M. Tsapatsis, Ultra-selective high-flux membranes from directly synthesized zeolite nanosheets. *Nature* **543**, 690–694 (2017).
27. L. Z. Wang, Y. Ebina, K. Takada, R. Kurashima, T. Sasaki, A new mesoporous manganese oxide pillared with double layers of alumina. *Adv. Mater.* **16**, 1412–1416 (2004).
28. S. L. Lawton, A. S. Fung, G. J. Kennedy, L. B. Alemany, C. D. Chang, G. H. Hatzikos, D. N. Lissy, M. K. Rubin, H.-K. C. Timken, S. Steuernagel, D. E. Woessner, Zeolite MCM-49: A three-dimensional MCM-22 analogue synthesized by in situ crystallization. *J. Phys. Chem.* **100**, 3788–3798 (1996).
29. R. C. Reynolds, Diffraction by small and disordered molecules, in *Modern Powder Diffraction*, D. L. Bish, J. E. Post, Eds. (Mineralogical Society of America, 1989), vol. 20, pp. 145–182.
30. G. W. Brindley, Order-disorder in clay mineral structures, in *Crystal Structures of Clay Minerals and their X-ray Identification*, G. W. Brindley, G. Brown, Eds. (Mineralogical Society, 1980), pp. 125–197.
31. D. E. W. Vaughan, Pillared clays - a historical perspective. *Catal. Today* **2**, 187–198 (1988).
32. W. J. Roth, C. T. Kresge, J. C. Vartuli, M. E. Leonowicz, A. S. Fung, S. B. McCullen, MCM-36: The first pillared molecular sieve with zeolite properties, in *Catalysis by Microporous Materials*, H. K. Beyer, H. G. Karge, I. Kiricsi, J. B. Nagy, Eds. (Elsevier, 1995), vol. 94, pp. 301–308.
33. S. Maheshwari, E. Jordan, S. Kumar, F. S. Bates, R. L. Penn, D. F. Shantz, M. Tsapatsis, Layer structure preservation during swelling, pillaring, and exfoliation of a zeolite precursor. *J. Am. Chem. Soc.* **130**, 1507–1516 (2008).
34. M. Thommes, Physical adsorption characterization of nanoporous materials. *Chem. Ing. Tech.* **82**, 1059–1073 (2010).
35. T. F. Degnan Jr., C. M. Smith, C. R. Venkat, Alkylation of aromatics with ethylene and propylene: Recent developments in commercial processes. *Appl. Catal. Gen.* **221**, 283–294 (2001).
36. R. C. Reynolds, Principles of powder diffraction, in *Modern Powder Diffraction*, D. L. Bish, J. E. Post, Eds. (Mineralogical Society of America, 1989), vol. 20, pp. 1–18.
37. C. T. Koch, "Determination of core structure periodicity and point defect density along dislocations," thesis, Arizona State University (2002).

Acknowledgments: We thank Y. Nemoto and Y. Yamauchi at NIMS for assistance in TEM analysis and SAXS measurements. **Funding:** This work was supported, in part, by the WPI-MANA, MEXT, Japan and JST CREST and JSPS KAKENHI projects (grant nos. JPMJCR17N1 and 15H02004), Japan. J.C. acknowledges the Czech Science Foundation (Project ExPro 19-27551X). J.C. and M.M. acknowledge support from OP VVV "Excellent Research Teams," project no. CZ.02.1.01/0.0/0.0/15_003/0000417–CUCAM. National Science Centre Poland grant nos. 2016/21/B/ST5/00858 (to J.G., B.G., and K.K.) and 2014/15/B/ST5/04498 (to W.J.R.) provided part of the funding. K.W. thanks the Foundation for Polish Science for the financial support (START 96.2018). **Author contributions:** W.J.R., T.S., and J.C. initiated the idea and coordinated synthesis and characterization studies and interpretation of results and writing. All authors were involved in data interpretation and writing. Basic preparations and characterization (Fourier transform infrared, powder XRD, nitrogen adsorption, and catalysis) were performed by W.J.R., B.G., J.G., and K.K. Advanced characterizations were carried out by K.W. and S.Z. (AFM). T.S., Y.S., D.-M.T., Y.E., and R.M. performed colloid preparation, SAXS, in situ XRD, TEM, and in-plane XRD. M.M. and J.C. performed the TEM of surfactant MWW. **Competing interests:** The authors declare that they have no competing interests. **Data and materials availability:** All data needed to evaluate the conclusions in the paper are present in the paper and/or the Supplementary Materials. Additional data related to this paper may be requested from the authors.

Submitted 20 July 2019
Accepted 20 December 2019
Published 20 March 2020
10.1126/sciadv.aay8163

Citation: W. J. Roth, T. Sasaki, K. Wolski, Y. Song, D.-M. Tang, Y. Ebina, R. Ma, J. Grzybek, K. Kałahurska, B. Gil, M. Mazur, S. Zapotoczny, J. Cejka, Liquid dispersions of zeolite monolayers with high catalytic activity prepared by soft-chemical exfoliation. *Sci. Adv.* **6**, eaay8163 (2020).

Liquid dispersions of zeolite monolayers with high catalytic activity prepared by soft-chemical exfoliation

Wieslaw J. Roth, Takayoshi Sasaki, Karol Wolski, Yeji Song, Dai-Ming Tang, Yasuo Ebina, Renzhi Ma, Justyna Grzybek, Katarzyna Kalahurska, Barbara Gil, Michal Mazur, Szczepan Zapotoczny and Jiri Cejka

Sci Adv **6** (12), eaay8163.
DOI: 10.1126/sciadv.aay8163